PERGAMON International Journal of Impact Engineering 25 (2001) 981–991

INTERNATIONAL JOURNAL OF IMPACT ENGINEERING

www.elsevier.com/locate/ijimpeng

Taylor impact test for ductile porous materials—Part 1: theory

Guoxing Lu[a,*], Bin Wang[b], Tieguang Zhang[c]

[a] *School of Engineering and Science, Swinburne University of Technology, Hawthorn, Victoria 3122, Australia*
[b] *Department of Mechanical Engineering, Brunel University, Uxbridge, Middlesex UB8 3PH, UK*
[c] *Institute of Applied Mechanics, Taiyuan University of Technology, Taiyuan 030024, People's Republic of China*

Received 26 May 2000; received in revised form 31 May 2001

Abstract

Taylor tests have been commonly employed to determine dynamic yield stress of solids at a high strain rate. In this paper, the original Taylor model is extended in order to provide a theoretical basis for testing ductile porous materials. The key difference between solids and porous materials in this respect is that porous materials are compressible and their density changes with the compressive strain. Calculations have been made for porous materials with a relative density that is a linear function of compressive strain e, i.e., $\rho/\rho_0 = 1 + ae$. The final length of the projectile after impact, L_1/L, is plotted against parameter $\rho_0 U^2/Y$ (see Fig. 9) and this plot is used in a Taylor test to determine the dynamic yield stress. The mean strain rate of the test can be estimated from Eqs. (21) or (22). In a companion paper (Int J Impact Eng), experiments for dynamic yield stress of porous materials will be reported based on the present theoretical analysis.

1. Introduction

Early in 1948, Taylor [1] and Whiffen [2] made investigations into the mushrooming of flat nosed cylindrical projectiles impinging rigid surfaces to study the effect of high strain-rates on dynamic yield strength of metals. The theoretical analysis by Taylor is well known as the Taylor model, and the corresponding Taylor test has become a standard procedure to determine dynamic yield stress of materials. In a Taylor test, strain-rate can reach as high as $10^4\,s^{-1}$, which is in the regime achievable between a Split–Hopkinson pressure bar and plate impact shear experiments.

Subsequently, several analyses for the Taylor test have been proposed in order to modify or to simplify the Taylor model. All these analyses are essentially based on the simple model employed

*Corresponding author. Fax: +61-3-9214-8264.
E-mail address: glu@groupwise.swin.edu.au (G. Lu).

0734-743X/01/$ - see front matter
PII: S0734-743X(01)00027-6

by Taylor, in which all plastic deformation is assumed to occur in a plastic wave front that moves towards the rear end of the projectile. Hawkyard et al. [3,4] reconsidered the Taylor model from the energy equilibrium rather than the momentum equilibrium across the plastic wave front adopted by Taylor. The mean dynamic yield stress evaluated by the energy equilibrium method was found to be higher than that by Taylor's theory, by 15% for mild steel, 20% for lead and 50% for copper. However, for armour plates, the mean dynamic yield stress evaluated by the energy equilibrium method was lower than by Taylor's theory by 4%. More recently, Jones et al. [5] proposed an elementary theory for the Taylor test. This elementary theory was based on an additional assumption that the speed of the plastic wave front is proportional to that of the undeformed section of the projectile.

In the original Taylor model, it was assumed that the material of the projectile is incompressible, i.e., its total volume does not change. The present paper extends Taylor's theory for the case of compressible materials, such as porous metals and metal foams. This research is particularly motivated by the recent development of porous materials and their potential applications in impact engineering due to their high energy absorption capacity. An important feature of porous material is that its density increases with compressive strain. This is a key point in the present analysis. The purpose of this paper is to provide an analysis that can be used in a Taylor test to determine the dynamic yield stress of ductile porous materials at a high strain-rate. Experiments for two porous materials at various strain-rates will be reported in a companion paper [6].

2. Problem and assumptions

Consider a short flat-nosed cylindrical projectile striking a flat rigid anvil at a normal angle with an initial velocity U (see Fig. 1(a)). Before impact, the projectile is of cross sectional area A_0, length L and material density ρ_0. Here a simplified deformation model of the projectile is used, similar to that employed by Taylor. The following five assumptions are made.

1. The pore size of the projectile material is much smaller than the diameter of the projectile; hence the material of projectile can be treated as a continuum.

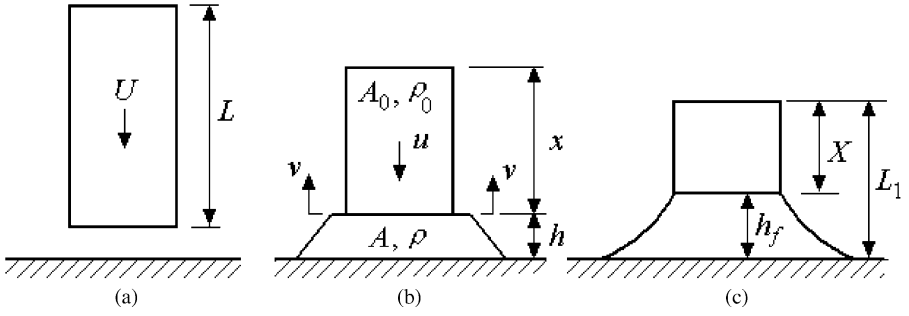

Fig. 1. A rigid-plastic projectile striking a rigid flat anvil at speed U: (a) before impact; (b) intermediate stage of deformation; and (c) final stage of deformation.

2. At time t during an intermediate stage of deformation, a steep-fronted plastic wave moves away from the anvil into the projectile at an absolute speed v (see Fig. 1(b)). The cross-sectional area across this wave front suddenly jumps from A_0 to A, and the projectile changes its density from ρ_0 to the current value, ρ.
3. The material, which has just passed through the plastic boundary, is brought to rest in a very short length; so a particle within the plastic deformed region remains stationary. The undeformed section of the projectile has an instantaneous absolute speed u.
4. The stress in the plastic deforming part of the projectile is constant, equal to the flow stress Y.
5. The relative density ρ/ρ_0 is a function of compressive strain only; it is independent of the strain rate.

3. Analysis

Essentially, Taylor's model is a problem with propagating strong discontinuity in velocity. The role of strong discontinuity in velocity has been discussed by Prager [7] for plates, by Hill [8] for three-dimensional continua, and by Zhang et al. [9] for beams. At a discontinuous surface, physical parameters must satisfy two basic equations: (1) the mass conservation equation, and (2) the momentum equation or dynamical equation in which a strong discontinuity in velocity is directly related to discontinuous stress resultants across the travelling surface. From the assumptions (1) and (2), rigid material of undeformed section of the projectile moves across the wave front with a speed $(u+v)$. The mass conservation equation across the plastic wave front is

$$\rho A v = \rho_0 A_0 (u+v). \tag{1}$$

At the wave front, the net force is $Y(A-A_0)$; the rate at which mass crosses the plastic wave front is $\rho_0 A_0 (u+v)$; and the jump in velocity at the plastic wave front is u. The momentum equation across the plastic wave front is

$$\rho_0 A_0 (u+v)u = Y(A-A_0). \tag{2}$$

The longitudinal engineering compressive strain at any point is defined as

$$e = 1 - \frac{A_0 \rho_0}{A\rho}. \tag{3}$$

Eliminating v from Eqs. (1) and (2), and using Eq. (3) to eliminate $A_0\rho_0$ and $A\rho$, we obtain

$$\frac{\rho_0 u^2}{Y} = e\left[\frac{\rho_0}{\rho(1-e)} - 1\right]. \tag{4}$$

The rate of change in undeformed length of the projectile is

$$\frac{\mathrm{d}x}{\mathrm{d}t} = -(u+v). \tag{5}$$

Considering the deceleration of the undeformed section of the projectile under retarding force YA_0, the equation of motion for the undeformed portion of the projectile is

$$\frac{\mathrm{d}u}{\mathrm{d}t} = -\frac{Y}{\rho_0 x}. \tag{6}$$

Eliminating $A_0\rho_0$ and $A\rho$ from Eqs. (1) and (3), it is found that $u+v=u/e$. From Eqs. (5) and (6) we have

$$\frac{\mathrm{d}x}{\mathrm{d}u}=\frac{\rho_0 x(u+v)}{Y}=\frac{\rho_0 xu}{Ye}. \tag{7}$$

Integrating Eq. (7) by considering Eq. (4)

$$\ln(x)^2=\int\frac{1}{e}\mathrm{d}\left[e\left(\frac{\rho_0}{\rho(1-e)}-1\right)\right]+C, \tag{8}$$

where C is an integration constant, and it can be determined from the initial condition. The rate of change in the length of the plastic zone is $\mathrm{d}h/\mathrm{d}t=v$, and from Eqs. (5), (1) and (3), we have

$$\frac{\mathrm{d}h}{\mathrm{d}x}=-\frac{v}{u+v}=-1+e.$$

Consequently

$$h=-\int_L^x(1-e)\,\mathrm{d}x. \tag{9}$$

The length of the plastic zone h can be obtained by numerical integration from Eq. (9).

It is clear that for a ductile porous material the relative density ρ/ρ_0 varies with compressive strain in a non-linear fashion. However, for the sake of simplicity, it is approximated here to be a linear function of compressive strain e (see Fig. 2):

$$\rho/\rho_0=1+ae, \tag{10}$$

where a is a relative density parameter, which can be obtained from a quasi-static compression test. Substituting Eq. (10) in Eqs. (4) and (8) we have

$$\frac{\rho_0 u^2}{Y}=e\left[\frac{1}{(1+ae)(1-e)}-1\right] \tag{11}$$

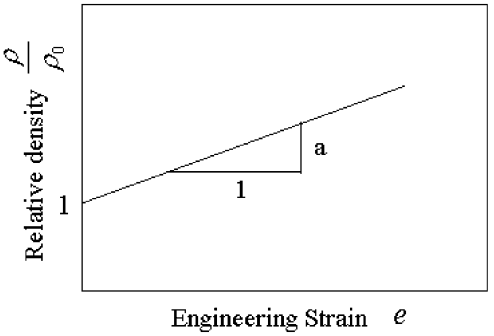

Fig. 2. Relative density versus compressive engineering strain.

and

$$\begin{aligned}\ln(x)^2 &= \int \frac{1}{e}\,\mathrm{d}\left[e\left(\frac{1}{(1+ae)(1-e)}-1\right)\right]+C,\\ &= \int \frac{1}{e}\left[\frac{1}{(1-e)(1+ae)}+\frac{e}{(1-e)^2(1+ae)}-\frac{ae}{(1-e)(1+ae)^2}-1\right]\mathrm{d}e+C,\\ &= \frac{1}{1+a}\left[\frac{1}{1-e}+\frac{a}{1+ae}-\ln(1-e)-a\ln(1+ae)\right]+C.\end{aligned} \tag{12}$$

After a Taylor test, the compressive strain e in the plastic deformation zone of the projectile decreases with distance from the contact surface. It has a maximum value, e_1, at the contact face and is zero at the interface between the deformed and undeformed sections of the projectile.

At the instant of impact, the length of undeformed section of the projectile is $x = L$ and the initial strain at the contact face is $e = e_1$, and so Eq. (12) becomes

$$\begin{aligned}\ln\left(\frac{x}{L}\right)^2 = \frac{1}{1+a}\Bigg[&\frac{1}{1-e}+\frac{a}{1+ae}-\ln(1-e)-a\ln(1+ae)\\ &-\frac{1}{1-e_1}-\frac{a}{1+ae_1}+\ln(1-e_1)+a\ln(1+ae_1)\Bigg].\end{aligned} \tag{13}$$

When the projectile is brought to rest, $x = X$ and $e = 0$ (see Fig. 1(c)), and the final length of the undeformed section of the projectile, X is

$$\ln\left(\frac{X}{L}\right)^2 = 1-\frac{1}{1+a}\left[\frac{1}{1-e_1}+\frac{a}{1+ae_1}-\ln(1-e_1)-a\ln(1+ae_1)\right]. \tag{14}$$

The time after initial impact, t, can be determined from Eqs. (6) and (11)

$$t = -\int \frac{\rho_0 x}{Y}\,\mathrm{d}u = -\int \frac{\rho_0 x}{Y}\sqrt{\frac{Y}{\rho_0}}\,\mathrm{d}\sqrt{e\left(\frac{1}{(1+ae)(1-e)}-1\right)}, \tag{15}$$

when $t = 0$, $u = U$ and $e = e_1$, from Eq. (11), we have

$$\frac{\rho_0 U^2}{Y} = e_1\left[\frac{1}{(1+ae_1)(1-e_1)}-1\right]. \tag{16}$$

Eliminating ρ_0/Y from Eqs. (15) and (16), the non-dimensional time is

$$\begin{aligned}\frac{tU}{L} = &-\left[\frac{e_1}{(1+ae_1)(1-e_1)}-e_1\right]^{\frac{1}{2}}\\ &\times\int_e^{e_1}\frac{x}{L}\frac{e/[(1-e)^2(1+ae)]+1/[(1-e)(1+ae)]-ae/[(1-e)(1+ae)^2]-1}{2\sqrt{e/[(1-e)(1+ae)]-e}}\,\mathrm{d}e.\end{aligned} \tag{17}$$

This deformation process of the projectile ends at time T_f, and its non-dimensional form is found from Eq. (17)

$$\frac{T_f U}{L} = -\left[\frac{e_1}{(1+ae_1)(1-e_1)} - e_1\right]^{\frac{1}{2}} \times \int_0^{e_1} \frac{x}{L} \frac{e/[(1-e)^2(1+ae)] + 1/[(1-e)(1+ae)] - ae/[(1-e)(1+ae)^2] - 1}{2\sqrt{e/[(1-e)(1+ae)] - e}} \,\mathrm{d}e. \tag{18}$$

At time T_f, the distance of the plastic boundary from the target plate is found from Eq. (9) (see Fig. 1(c)), that is

$$h_f = -\int_L^X (1-e)\,\mathrm{d}x. \tag{19}$$

The final length of the projectile after impact is

$$L_1 = X + h_f. \tag{20}$$

4. Numerical procedure

Calculations have been carried out for several values of the initial strain e_1 and relative density parameter a. The procedure for a numerical solution is as follows, which is repeated for different values of initial strain:

1. For an assumed initial strain e_1, select a strain step equal to, say, $\Delta e = e_1/20$.
2. Using Eq. (13), calculate the non-dimensional length of the undeformed section of the projectile, x/L, for the range of e from 0 to e_1, while the final length of the undeformed section of the projectile x/L is worked out from Eq. (14). The small increment of non-dimensional length $\Delta(x/L)$ is recorded for each step Δe.
3. With the aid of x/L obtained from the last step, numerically integrate Eq. (9) for the non-dimensional length of the plastic zone h/L for the range of e from 0 to e_1, and the small increment of the non-dimensional length $\Delta(h/L)$ is recorded for each step Δe. The final length of h_f is found.
4. The non-dimensional time tU/L is numerically integrated from Eq. (17) for the range of e from 0 to e_1, and the small increment of the non-dimensional time $\Delta(tU/L)$ is recorded for each step Δe. The non-dimensional time T_f is found finally.
5. The non-dimensional travelling speed of the plastic wave v/U is calculated by dividing $\Delta(h/L)$ by $\Delta(tU/L)$. The non-dimensional speed of the undeformed section of the projectile u/U is calculated by the formula $u/U = -[(\Delta x/L) - (\Delta h/L)]/[\Delta tU/L]$.
6. The final length of the projectile after impact is calculated from Eq. (20), and the non-dimensional parameter $\rho_0 U^2/Y$ is calculated from Eq. (16).

5. Results and discussion

Calculations are made for initial strain $e_1 = 0.3,\ 0.5$ and 0.7, and for relative density parameter $a = 0,\ 0.5,\ 0.8$ and 1. The relationship between the non-dimensional time Ut/L and the non-dimensional length of the undeformed section of projectile x/L, and that between Ut/L and the non-dimensional length of the plastic zone h/L are shown, respectively, in Fig. 3 for $e_1 = 0.3$, Fig. 4 for $e_1 = 0.5$ and Fig. 5 for $e_1 = 0.7$. The tip of the curves in each figure corresponds to the value of the final length of the undeformed section of the projectile x/L and the final distance of the plastic boundary from the target plate (h_f/L) at time T_f. From Figs. 3–5, it is found that for a given initial strain e_1, the final length of the undeformed section of the projectile x/L increases with increase in the relative density parameter a. Also, the final distance of the plastic boundary from the target plate h_f/L decreases with increasing the relative density parameter a. It seems that for a given value of the initial strain e_1, when the value of the relative density parameter is high, plastic deformation is concentrated in the small vicinity of impact face.

The relationship between the non-dimensional time Ut/L and the non-dimensional velocity of the undeformed section of projectile u/U is shown in Fig. 6(a) for $e_1 = 0.3$, Fig. 7(a) for $e_1 = 0.5$

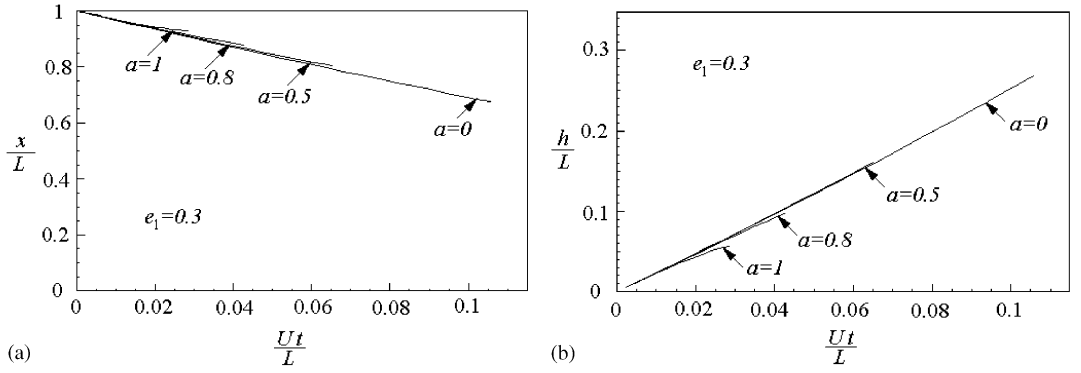

Fig. 3. Length of undeformed section of projectile and propagation of plastic boundary for initial strain $e_1 = 0.3$.

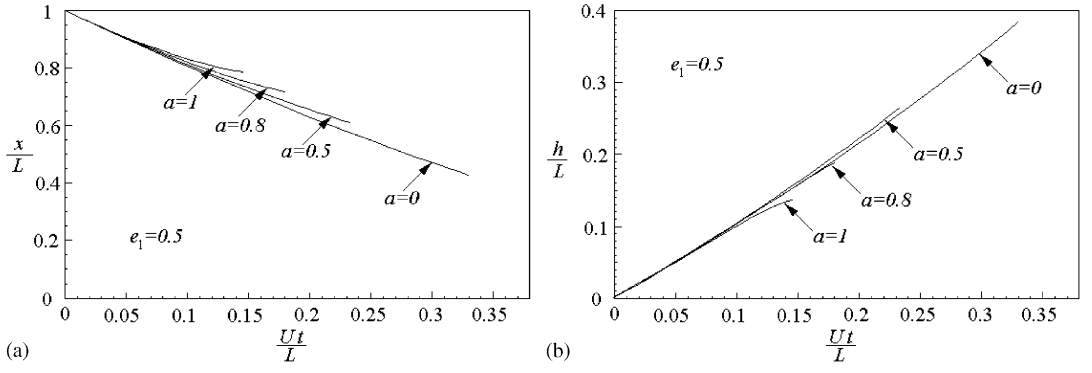

Fig. 4. Length of undeformed section of projectile and propagation of plastic boundary for initial strain $e_1 = 0.5$.

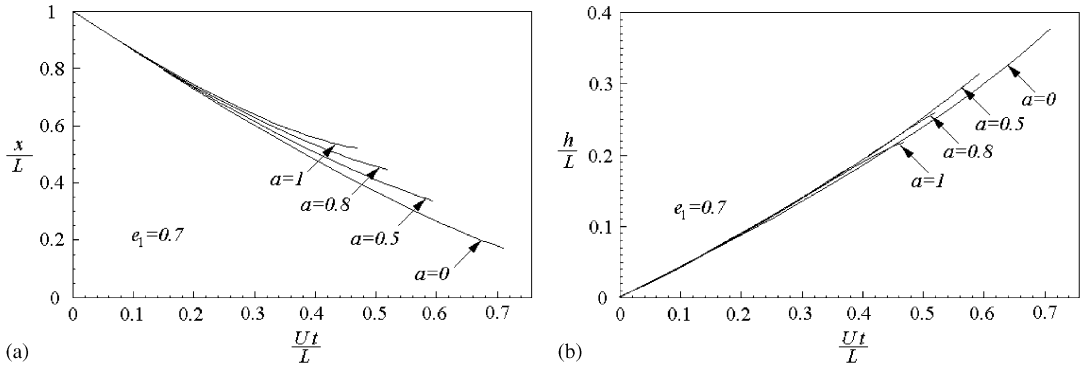

Fig. 5. Length of undeformed section of projectile and propagation of plastic boundary for initial strain $e_1 = 0.7$.

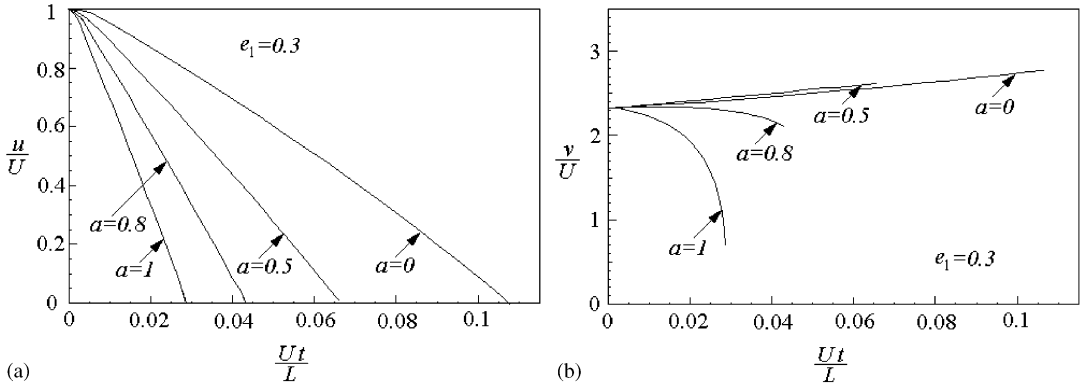

Fig. 6. Velocity of undeformed section of projectile and plastic wave velocity for initial strain $e_1 = 0.3$.

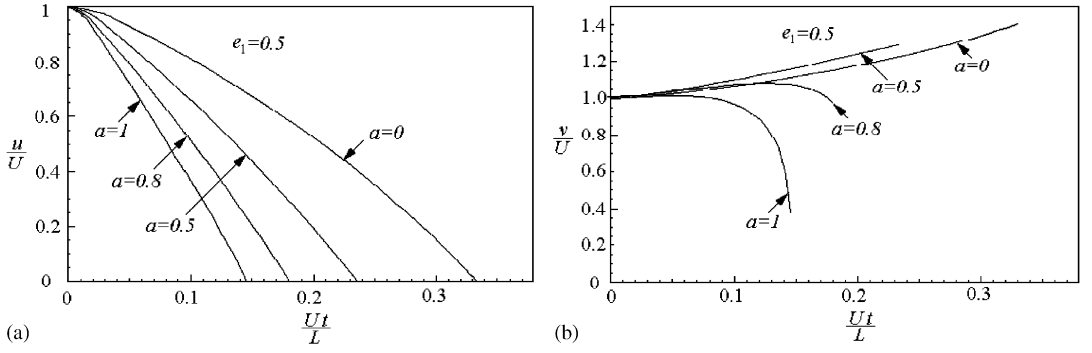

Fig. 7. Velocity of undeformed section of projectile and plastic wave velocity for initial strain $e_1 = 0.5$.

and Fig. 8(a) for $e_1 = 0.7$. The slope of the curves in these plots show the decelerations of the undeformed section. The rate of the deceleration is increasing with time, especially for a large value of the initial strain. Non-dimensional velocity of propagation of the plastic wave against the non-dimensional time is shown in Fig. 6(b) for $e_1 = 0.3$, Fig. 7(b) for $e_1 = 0.5$ and Fig. 8(c) for

$e_1 = 0.7$. For a small value of the relative density parameter, say $a = 0$ or 0.5, the propagation velocity of the plastic wave steadily increases with time. However, for a large value of the relative density parameter, such as $a = 0.8$ or 1, the propagation velocity of the plastic wave falls after a certain period of time. For a given initial strain e_1, this drop of the propagation velocity of the plastic wave for materials with a large value of a means that plastic deformation zone is more localised than with a small one, which has been shown in Figs. 3–5.

Calculated values of the non-dimensional final length of the projectile L_1/L and the non-dimensional final length of the plastic deformation zone $h_f/L = (L_1 - X)/L$ are plotted in Fig. 9 against the parameter $\rho_0 U^2/Y$ for the relative density parameter $a = 0$, 0.5 and 1. For a given value of parameter $\rho_0 U^2/Y$, both L_1/L and $(L_1 - X)/L$ decrease with the relative density parameter a. Since the final length of the projectile L_1 is easy to measure in a Taylor impact test, L_1/L versus $\rho_0 U^2/Y$ curve is used in determining parameter value of $\rho_0 U^2/Y$ for a given value of L_1/L, from which the dynamic yield stress is calculated.

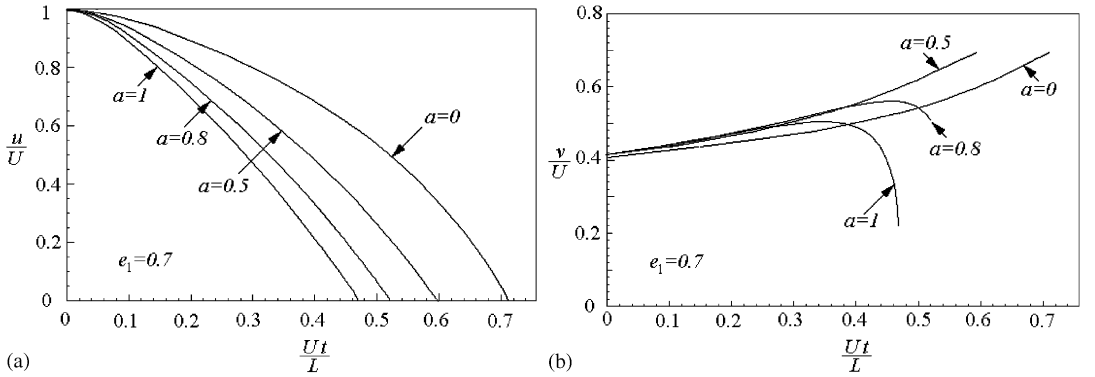

Fig. 8. Velocity of undeformed section of projectile and plastic wave velocity for initial strain $e_1 = 0.7$.

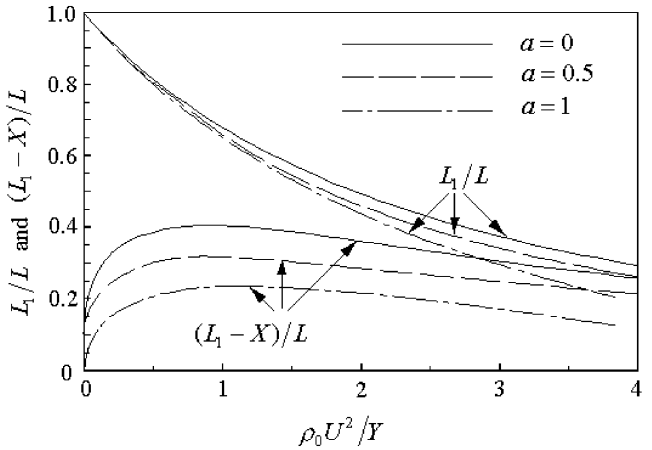

Fig. 9. Final projectile overall length and deformed length for several values of the relative density parameter.

Table 1
Mean strain rate $\dot{\varepsilon}_m L/U$ and $\dot{\varepsilon}_{mT} L/U$

Initial strain	Relative density parameter	$\frac{\dot{\varepsilon}_m L}{U}$	$\frac{\dot{\varepsilon}_{mT} L}{U}$	$\frac{\dot{\varepsilon}_m - \dot{\varepsilon}_{mT}}{\dot{\varepsilon}_{mT}}$ (%)
$e_1 = 0.3$	$a = 0$	1.64	1.54	6.5
	$a = 0.5$	2.66	2.57	3.6
	$a = 0.8$	4.27	4.18	2.1
	$a = 1$	7.20	7.10	1.5
$e_1 = 0.5$	$a = 0$	1.00	0.88	13.8
	$a = 0.5$	1.39	1.28	8.1
	$a = 0.8$	1.87	1.77	5.5
	$a = 1$	2.45	2.36	4.2
$e_1 = 0.7$	$a = 0$	0.77	0.60	27.6
	$a = 0.5$	0.88	0.75	17.4
	$a = 0.8$	1.02	0.91	13.0
	$a = 1$	1.16	1.05	10.8

The value of the strain rate is estimated as follows. The reduction in projectile length is $(L - L_1)$, and this is entirely confined to the material with an initial length $(L - X)$. The mean plastic strain is therefore $(L - L_1)/(L - X)$. The mean rate of strain is defined as

$$\dot{\varepsilon}_m = \frac{(L - L_1)}{(L - X)} \frac{1}{T_f}. \tag{21}$$

Taylor [1] suggested a simple method to estimate the mean strain rate on the assumption that the deceleration of the projectile is uniform. As the duration of deformation process is $2(L - L_1)/U$, the mean rate of strains estimated by Taylor is

$$\dot{\varepsilon}_{mT} = \frac{U}{2(L - X)}. \tag{22}$$

Calculated values of the non-dimensional mean strain rate $\dot{\varepsilon}_m L/U$ and $\dot{\varepsilon}_{mT} L/U$ are listed in Table 1. From the above discussion for Figs. 6–8, the rate of deceleration for the undeformed section of the projectile is not uniform, but is increasing with time. Hence Eq. (22) underestimates the mean strain rate. From Table 1, it can be seen that the discrepancy in mean strain rate estimated from Eqs. (21) and (22) increases with the initial strain e_1, and it decreases with the relative density parameter a. For a large value of the initial strain, say $e_1 = 0.7$, the mean strain rate from Eq. (21) is 27.6% higher than that from Eq. (22) for $a = 0$; and it is 10.8% for $a = 1$.

6. Conclusions

In this paper, the Taylor model has been extended in order to provide a theoretical basis for determining, by means of a Taylor test, dynamic flow stress of ductile porous materials at high strain rates. Calculations have been made for porous materials, of which the relative density is assumed to be a linear function of compressive strain e, i.e. $\rho/\rho_0 = 1 + ae$. It is found that, for a

given value of the initial strain e_1, when the value of a increases, plastic deformation tends to be confined within a narrow section near the impact surface. The curve of L_1/L versus $\rho_0 U^2/Y$ in Fig. 9 is used in the present modified Taylor test to determine the dynamic flow stress. The mean strain rate can be estimated from Eqs. (21) or (22). For a high value of the initial strain e_1, the mean strain rate predicted from Eq. (22) is about 10% lower than that from Eq. (21).

Acknowledgements

The authors wish to acknowledge the financial support for this work by an Australian Research Council Large Grant Scheme.

References

[1] Taylor GI. The use of flat-ended projectiles for determining dynamic yield stress I: theoretical considerations. Proc R Soc London A 1948;194:289–99.
[2] Whiffen AC. The use of flat-ended projectiles for determining dynamic yield stress II: tests on various metallic materials. Proc R. Soc London A 1948;194:300–22.
[3] Hawkyard JB, Eaton D, Johnson W. The mean dynamic yield strength of copper and low carbon steel at elevated temperatures from measurements of the mushrooming of flat-ended projectiles. Int J Mech Sci 1968;10:929–48.
[4] Hawkyard JB. A theory for the mushrooming of flat-ended projectiles impinging on a flat rigid anvil, using energy consideration. Int J Mech Sci 1969;11:313–33.
[5] Jones SE, Drinkard AJ, Rule WK, Wilson LL. An elementary theory for the Taylor impact test. Int J Impact Eng 1998;21:1–13.
[6] Zhang J, Wang B, Lu G. Taylor impact test for ductile porous materials—part 2: experiments. Int J Impact Eng, to be submitted.
[7] Prager W. Discontinuous fields of plastic stress and flow. Proceedings of the second US National Congress of Applied Mechanics. ASME, New York, 1954. p. 21–32.
[8] Hill R. Discontinuity relations in mechanics of solids. Progress Sol Mech II, 1961;247–76.
[9] Zhang TG, Stronge WJ, Yu TX. Dynamic deformation of rigid-plastic beams under general impulsive loading: a phenomenological model. Int J Impact Eng 1995;16:535–62.